

NJC

New Journal of Chemistry

Accepted Manuscript

A journal for new directions in chemistry

This article can be cited before page numbers have been issued, to do this please use: G. Fernández Freixes, L. Bernardo López, A. Villanueva and R. Pleixats, *New J. Chem.*, 2020, DOI: 10.1039/D0NJ00284D.



This is an Accepted Manuscript, which has been through the Royal Society of Chemistry peer review process and has been accepted for publication.

Accepted Manuscripts are published online shortly after acceptance, before technical editing, formatting and proof reading. Using this free service, authors can make their results available to the community, in citable form, before we publish the edited article. We will replace this Accepted Manuscript with the edited and formatted Advance Article as soon as it is available.

You can find more information about Accepted Manuscripts in the [Information for Authors](#).

Please note that technical editing may introduce minor changes to the text and/or graphics, which may alter content. The journal's standard [Terms & Conditions](#) and the [Ethical guidelines](#) still apply. In no event shall the Royal Society of Chemistry be held responsible for any errors or omissions in this Accepted Manuscript or any consequences arising from the use of any information it contains.

ARTICLE

Gold nanoparticles stabilized by PEG-tagged imidazolium salts as recyclable catalysts for the synthesis of propargylamines and the cycloisomerization of γ -alkynoic acidsReceived 00th January 20xx,
Accepted 00th January 20xx

DOI: 10.1039/x0xx00000x

Guillem Fernández,^a Laura Bernardo,^a Ana Villanueva,^a and Roser Pleixats^{*a}

We report the synthesis of PEGylated imidazolium (bromide and tetrafluoroborate) and tris-imidazolium (bromide) salts containing triazole linkers, and their use as stabilizers for the preparation of water-soluble gold nanoparticles by reduction of tetrachloroauric acid with sodium borohydride. The nanomaterials have been characterized. The X-Ray Photoelectron Spectroscopy (XPS) indicated the presence of Au(I) and Au(0) species, the oxidized form being more abundant in the nanomaterial derived from the tris-imidazolium bromide. The catalytic activity of these gold nanoparticles has been proved in the A³ coupling between carbonyl compounds, terminal alkynes and amines to afford propargylamines, and in the cycloisomerization of γ -alkynoic acids to enol lactones. The nanomaterial derived from the PEG-tagged tris-imidazolium bromide provided the best performance and it has been recycled in both reactions (up to four and six runs) taking advantage of its solubility properties.

Introduction

The studies on the synthesis, properties and potential applications of gold nanoparticles (Au NPs) have provided an exponentially increasing number of publications in the last two decades. The huge research efforts of the chemical community on this type of nanomaterials are mostly due to the particular stability, low toxicity and biocompatibility of Au NPs as well as to their size-related electronic and optical properties (quantum-size effect) and their high surface-to-volume ratio. Thus, applications in diverse areas have been described, such as biomedicine,¹ chemical and biological sensing,² and catalysis.³ In the field of catalysis, gold nanoparticles have been mainly reported for selective hydrogenations and other reduction reactions,^{3a-f, 3h-l, 3k} and for oxidative transformations.^{3a, 3c-d, 3f-g, 3j} Other less explored processes include C-C coupling,^{3c-d, 3f-g, 3k-l} hydrosilylation^{3f} and alkyne activation.^{3b, 3f-g, 3l-m}

Small-size metal nanoparticles are generally expected to give better catalytic performance⁴ because of the higher surface area, maximizing the fraction of metal atoms on the surface of the nanocatalyst. However, thermodynamics favour the bulk metal and facile aggregation of the nanoparticles occurs in solution, which lead to diminished catalytic activity over time. The main strategy to overcome this problem consists in supporting the gold nanoparticles in a suitable inorganic matrix.^{3a, 3e, 3h-k} Less common in the case of gold is the avoidance of the agglomeration of soluble colloids with

effective stabilizers added during the preparation process,^{3d, 5} including polymers.⁶ The nature of the protecting agent determines the solubility of the gold nanoparticles. Thus, a suitable choice of the stabilizer may provide Au NP soluble in organic, fluoruous or aqueous medium and may even enable the recycling.

Our group has been interested in the catalytic applications of soluble metal nanoparticles. In this sense, we have reported palladium,⁷ nickel⁸ and platinum⁹ nanoparticles stabilized by tris-imidazolium salts bearing long hexadecyl chains soluble in some organic solvents as catalysts for C-C bond forming reactions,^{7a-b} selective reduction of nitroarenes⁸ and stereoselective hydrosilylation of internal alkynes.^{7c, 9} However, we were not able to find a reproducible and satisfactory protocol for the obtention of gold nanoparticles with these type of stabilizers. Moreover, we have also developed PEG-tagged stabilizers using copper-catalyzed azide-alkyne cycloaddition (CuAAC) chemistry, which have been used in the preparation of water-soluble palladium nanoparticles¹⁰ for cross-coupling reactions, rhodium nanoparticles¹¹ for the hydrosilylation of alkynes and gold nanoparticles¹² for the reduction of nitroarenes. The polyoxyethylenated substrates featured three PEG chains bound to a central three-fold symmetric core with a benzene¹⁰ or triazine^{11, 12} ring in the center of the core.

Then, we have envisaged the design of new substrates for the stabilization of gold nanoparticles that combine some structural features of both types of the aforementioned capping agents, namely imidazolium and tris-imidazolium salts bearing polyoxyethylenated chains through triazole-containing linkers (**S1A-B** and **S2** in Figure 1). The imidazolium moieties would provide electrostatic interactions and coordinating nitrogens of triazole rings would enhance the stabilizing properties. Moreover, the hydrophilic PEGylated counterparts would contribute to the electrosteric stabilization and to the tuning of the solubility of the substrates and

^aG. Fernández, L. Bernardo, A. Villanueva, Prof. R. Pleixats. Department of Chemistry and Centro de Innovación en Química Avanzada (ORFEO-CINQA) Universitat Autònoma de Barcelona 08193-Cerdanyola del Vallès (Barcelona) (Spain) E-mail: roser.pleixats@uab.cat.

Electronic Supplementary Information (ESI) available: [details of any supplementary information available should be included here]. See DOI: 10.1039/x0xx00000x

ARTICLE

Journal Name

the resulting metal nanoparticles (solubility in water, insolubility in diethyl ether).

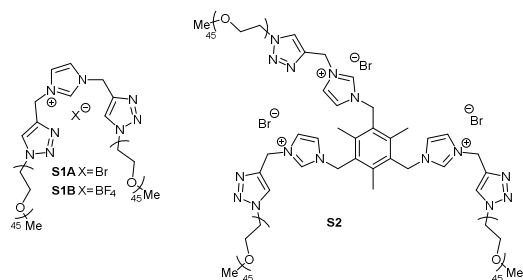


Figure 1. PEG-tagged imidazolium salts as stabilizers for gold nanoparticles

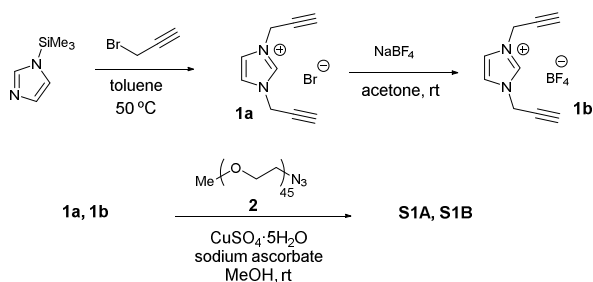
We present herein the synthesis of the stabilizers **S1A-B** and **S2**, the preparation and characterization of gold nanoparticles and their use as recyclable catalysts in two organic transformations, namely the A^3 coupling between aldehydes, terminal alkynes and amines to afford propargylamines, and the cycloisomerization of γ -alkynoic acids to enol lactones, less explored with Au NPs than other types of reactions.^{3b, 3f, 3l-m}

Stabilizers **S1A** and **S1B** were designed in order to explore the effect of two different counteranions for the same imidazolium cation, and the bromides **S1A** and **S2** would allow us to investigate the effect of the cation.

Results and Discussion

Preparation of PEG-tagged imidazolium salts

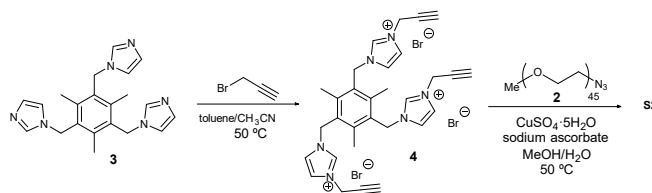
The synthesis of the stabilizers **S1A-B** (Figure 1, bromide and tetrafluoroborate as counter anion, respectively) is summarized in Scheme 1.



Scheme 1. Preparation of PEG-tagged imidazolium salts **S1A-B**.

A mixture of *N*-(trimethylsilyl)imidazole and excess of propargyl bromide was heated in toluene at 50 °C following a described method¹³ affording **1a** as an hygroscopic solid (94%). Treatment of this imidazolium bromide with sodium tetrafluoroborate in acetone at room temperature gave the imidazolium tetrafluoroborate **1b** (91%).¹³ Finally, **S1A-B** were obtained (86 and 84% yield, respectively) through a copper-catalyzed [3+2] cycloaddition reaction¹⁴ between the alkyne-derivatized imidazolium salts **1a-b** and the PEGylated azide **2**^{10b},¹¹ in methanol at room temperature by a modification of a described procedure.¹⁵

On the other hand, the synthesis of the PEG-tagged tris-imidazolium salt **S2** was accomplished as outlined in Scheme 2.



Scheme 2. Preparation of PEG-tagged tris-imidazolium salt **S2**.

The reaction of the C_3 -symmetric tris-imidazole **3**^{16, 7a} with excess of propargyl bromide in a 2:1 mixture of toluene/acetonitrile at 50 °C afforded the tris-imidazolium salt **4** (63%) as an hygroscopic solid. It was insoluble in dichloromethane, chloroform, acetone, diethyl ether and acetonitrile, slightly soluble in ethanol and methanol, and very soluble in water and dimethyl sulfoxide. A three-fold copper-catalyzed azide-alkyne cycloaddition (CuAAC) between the trialkyne **4** and the azide **2** in methanol/water 1:1 at 50 °C was performed to give the desired stabilizer **S2** (79%).

Preparation and characterization of gold nanoparticles

The bottom-up procedures are preferred over the top-down approach for the formation of Au NPs, the former consisting mainly of chemical methods,^{3k, 17} with the reduction of gold salts being the most common.

Imidazolium salts have been described as capping agents in the synthesis of Au NPs.¹⁸ In order to enhance the stabilizing properties, very often coordinating groups (amino, thiol,...) are introduced in the cationic moiety or the imidazolium salt is part of a polymer. NHC-protected gold nanoparticles have also been reported,^{15, 19} which were obtained from organometallic NHC-Au(I) complexes^{15, 19b, 19e-g} or by using *N*-heterocyclic carbenes (NHC), *in situ* or previously formed from the corresponding imidazolium salts.^{19c, 19d, 19h}

We have prepared gold nanoparticles by a chemical reduction of tetrachloroauric acid trihydrate with sodium borohydride in water at room temperature in the presence of the corresponding stabilizer **S1A-B** or **S2** (entries 1-3, Table 1). In all cases a molar ratio Au:S of 1:0.3 was used, which was found convenient for other type of PEG-tagged ligands.¹² Upon addition of an excess of $NaBH_4$ (6.7 mol per mol of Au), the reaction mixture underwent a colour change from light yellow to dark red. No precipitate of bulk gold was formed after stirring overnight. After filtration of the reaction mixture through a Millipore filter, the filtrate was extracted with dichloromethane. Upon removal of the solvent, the corresponding nanomaterial was obtained as a dark maroon solid. The Au NPs were soluble in water, tetrahydrofuran, dichloromethane and chloroform and insoluble in diethyl ether and hexane.

TEM analysis confirmed the formation of spherical and well-dispersed nanoparticles of mean diameters from 4.5 to 5.6 (entries 1-3, Table 1). Selected TEM and high-resolution (HR) TEM micrographs, and the corresponding size distributions histograms of the materials are shown in Figure 2. The yield with respect to the initial amount of Au used was calculated on the basis of elemental

analysis of gold in the nanomaterials (inductively coupled plasma, ICP) (Table 1).

View Article Online
DOI: 10.1039/D0NJ00284D

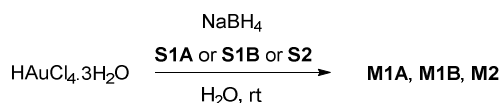


Table 1. Preparation of Au NPs stabilized by **S1A-B** and **S2**.^[a]

Entry	S	Diameter ^[b] (nm)	% Au		Yield ^[d] (%)	Nanomaterial
			theor	expt ^[c]		
1	S1A	5.2 ± 3	11.6	10.9	79	M1A
2	S1B	4.5 ± 2	11.6	9.5	69	M1B
3	S2	5.6 ± 1.5	7.5	6.9	69	M2
4 ^[e]	S2	3.3 ± 1.4	7.5	8.2	74	M2'

[a] Molar ratio Au:S:NaBH₄ = 1: 0.3: 6.7; [Au] = 0.6 mM. [b] Mean diameter by TEM. [c] Determined by ICP. [d] Based on amount of HAuCl₄ used. [e] Molar ratio Au:S:NaBH₄ = 1: 0.3: 20.

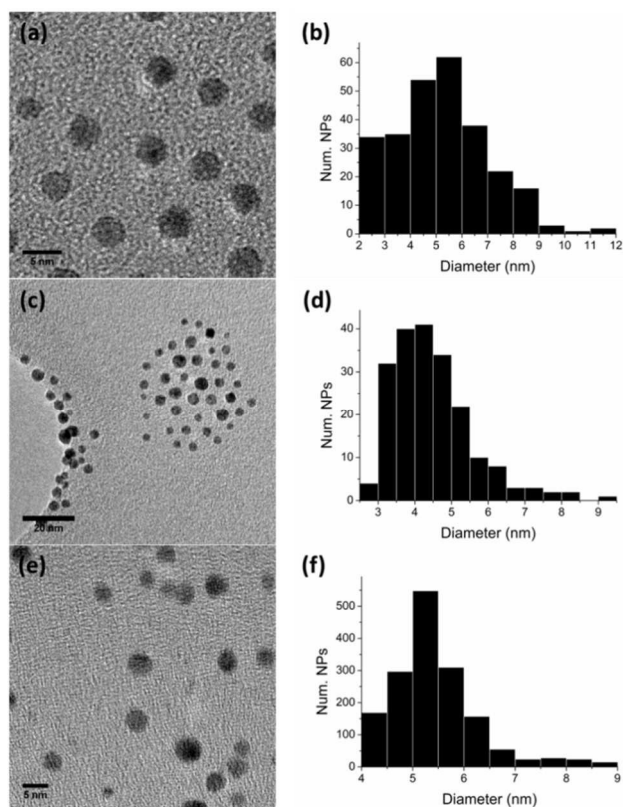


Figure 2. TEM images and the corresponding size distribution histograms of materials (a)-(b) **M1A**, (c)-(d) **M1B**, (e)-(f) **M2**

The Energy-Dispersive X-ray Spectroscopy (EDS) data of **M1B** is given as a representative example in Figure 3 and confirms the presence of gold.

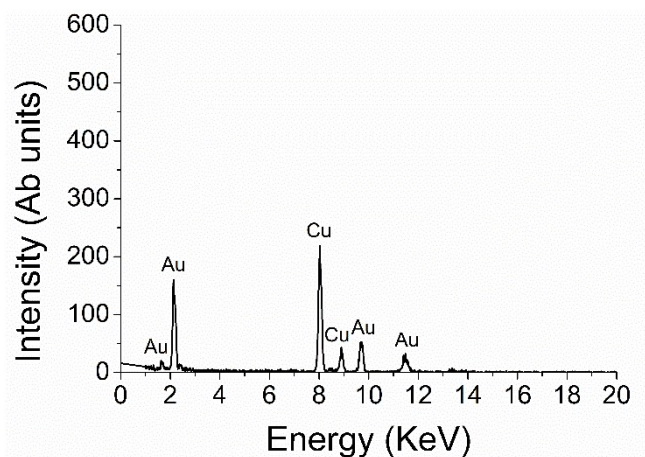


Figure 3. EDS spectrum of Au NPs (**M1B**).

The experimental interplanar distances measured by electron diffraction (ED) were close to those expected for the face-centered cubic (fcc) gold lattice (Table 2).

Table 2. Electron diffraction pattern of **M1B**

h k l	d _{hkl} (nm)	
	Exper.	Theor.
(111)	0.2293	0.2355
(200)	0.2040	0.2040
(220)	0.1426	0.1442
(311)	0.1203	0.1230

However, the X-ray photoelectron spectrum (XPS) of the material **M2** in the Au 4f region (Figure 4) indicated a mixture of two valence states of gold. It exhibited a doublet at 83.8 and 87.5 eV for the Au 4f_{7/2} and Au 4f_{5/2}, respectively, corresponding to Au(0).²⁰ Additionally, another doublet at 85.1 and 88.8 eV is attributed to Au 4f_{7/2} and Au 4f_{5/2} of Au(I).^{20a} Considering the possibility that not all the gold(III) had been completely reduced, although an excess of sodium borohydride was used, we performed a similar experiment but adding a much higher amount of NaBH₄ (20 mol per mol of Au)^{18g} to obtain **M2'**. These Au NPs gave a mean particle size of 3.3 nm and a gold content of 8.2% by ICP-OES (entry 4, Table 1; see TEM image and size distribution histogram of **M2'** in figure S1 of supporting information). Unexpectedly, the XPS spectrum of **M2'** was similar to that of **M2** and displayed signals for both Au(I) and Au(0) species, even with slightly higher intensity of Au(I) doublet with respect to that corresponding to Au(0). In contrast, according to the XPS spectra of **M1A** and **M1B**, both species were present in these nanomaterials, but Au(0) predominated (see XPS spectra of **M2'**, **M1A**, **M1B** in figure S2 in supporting information). Alternative

explanations for the observation of Au⁺ species in XPS should then arise. One of them would be the formation of an oxidized layer on the surface of the particles. It has been described that the surface of some imidazolium ionic liquids-stabilized metal nanoparticles is more susceptible to oxidation in air than the bulk metal, the presence of such oxidized layer enhancing the stability of the particles.²¹ Another option is the formation of Au(I) nanoparticles, species which have been described to be produced *in situ* from the reduction of an Au(III) complex in a catalytic A³ coupling reaction.^{20a} A third possibility is the generation of a gold(I) complex of type NHC-Au-X through deprotonation of the acidic hydrogen at the C2 position of the imidazolium moiety by a hydride anion of the reducing agent used in excess. The resulting NHC ligand would coordinate to Au(I) intermediate derived from partial reduction of the gold(III) precursor. Although NaBH₄ has been reported by some authors to reduce NHC-Au(I) complexes to the corresponding NHC-stabilized Au NP,^{19e-f} a recent article^{19g} describes the presence of Au(0) and Au(I) species by XPS after treatment of the complex with excess of this reducing agent (20 mol-equiv). In that case, the values of Au 4f signals for the NHC-Au-Cl complex (86.3 and 90.0 eV) and the formed NHC-Au(I) NPs (86.2 and 89.9 eV) do not differ significantly, but as they could not detect a significant amount of Cl by XPS, they discard the presence of the complex. The exact nature of these Au(I) species still remains unsolved.^{19g} In the present work, we have detected signals of Cl 2p in the XPS of **M2** (which were not clearly seen in **M2'**) that would have the origin on the gold precursor (see figure S3 in supporting information). We could not clearly identify Br by XPS neither in the nanomaterials **M2/M1A** nor in the stabilizers **S2/S1A**, probably due to the low percentage of this element in the high molecular weight stabilizers. On the other hand, XPS of the N 1s has been claimed to evidence the formation of NHC-capped Au(0) nanoparticles from the reduction of imidazolium-AuX₄ salts with NaBH₄ (a shift from 401.6 for imidazolium bromide to 400.2 for the Au NPs capped by NHC).^{19h} In our case, the N1s photopeaks were very weak and the smaller differences in the positions of the signals makes it difficult to draw conclusions.

On the other hand, the counterion effect was evident in the appearance of the ¹H NMR spectra of the Au NPs **M1A** and **M2** derived from the bromide salts **S1A** and **S2**, respectively, and **M1B** derived from the tetrafluoroborate **S1B** (see figure S4 in supporting information). Only the signals of methyl and methylene groups of the PEGylated chains were clearly observed in **M1A** and **M2** (and also in **M2'**). In contrast, the ¹H NMR spectrum of **M1B** presented all the absorptions of the free stabilizer, including the proton at C2 of the imidazolium ring appearing at 9.12 ppm, but the signals of the other protons of imidazole, triazole and the methylene group between both rings are splitted. The broadening and disappearance of absorptions of some protons would be in line with a stronger stabilizer-metal surface interaction in the case of bromide salts.²² This indicates that the heterocycle is close to the surface of the metal, but it is not conclusive with respect to its nature: imidazolium or carbene. We observed a similar phenomenon in the ¹H NMR spectra of Pd NPs stabilized by iodide and tetrafluoroborate tris-imidazolium salts containing hexadecyl chains.^{7a}

Thus, the formation of a mixture of Au(0) and Au(I) NPs seems more likely in our case, but we cannot conclusively rule out the presence of a certain amount of NHC-Au-Cl complex in **M2**.

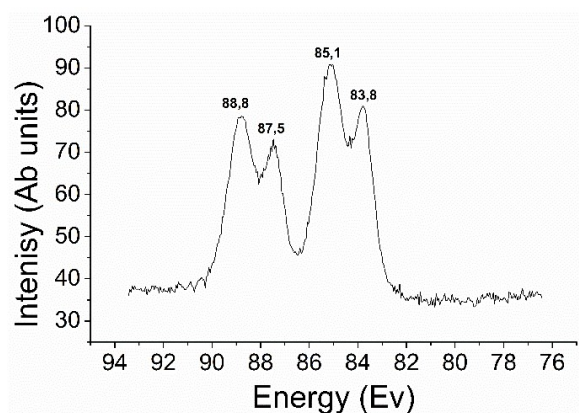


Figure 4. XPS spectrum of **M2** in the Au 4f region.

In the UV-Vis spectra of all the Au NPs, we observed the appearance of a broad shoulder (centered at 519 nm for **M2**) representing the localized surface plasmon resonance (LSPR) band (Figure 5).

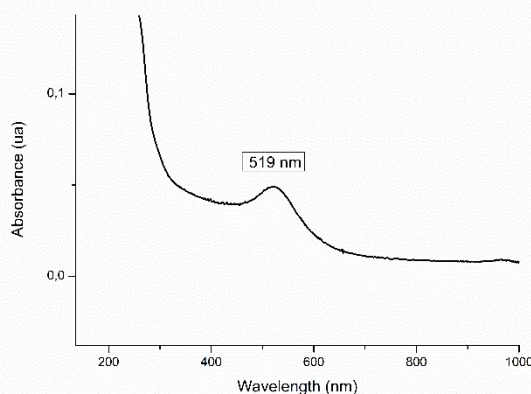


Figure 5. LSPR band in the UV-Vis spectrum of **M2**.

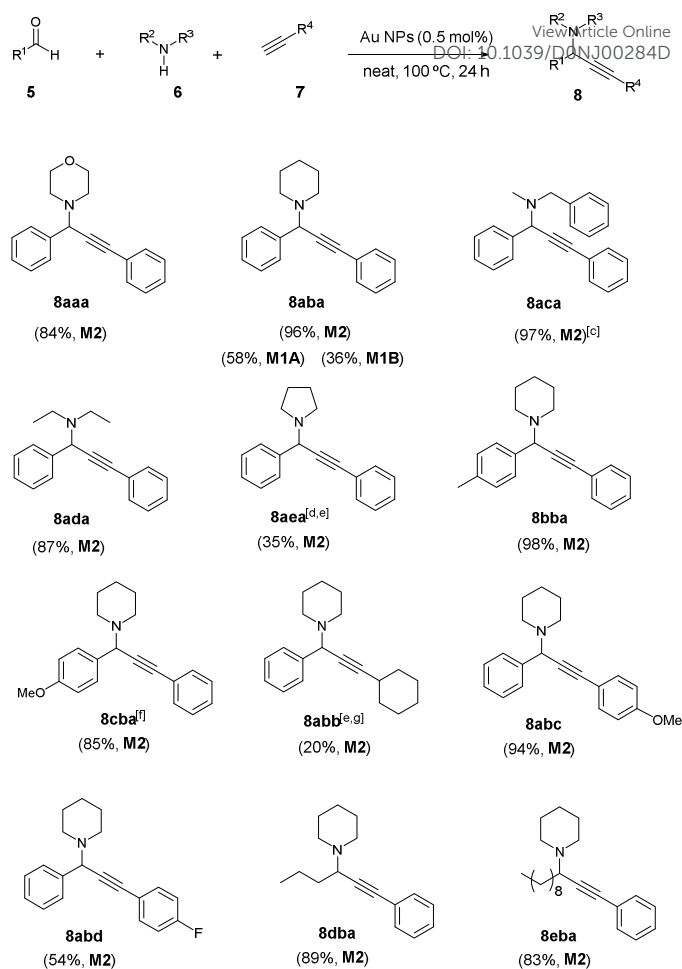
Activity of gold nanoparticles in the synthesis of propargylamines by a three-component coupling reaction

Propargylamines²³ are valuable and versatile synthetic building blocks for the preparation of several types of N-containing heterocycles²⁴ and for the manufacturing of natural and pharmaceutical products.²⁵ The conventional method for the synthesis of propargylamines consists in the nucleophilic attack of lithium acetylides (or the Grignard reagents) to imines. To avoid the use of stoichiometric organometallic reagents, which require strictly moisture-free conditions and the protection of sensitive functional groups, an alternative atom-economical approach has been developed, namely the catalytic three-component reaction between aldehydes, amines and terminal alkynes (A³ coupling).²⁶ Catalysis of this transformation by Au(I) or Au(III) species has been documented,^{3b,20a,26,27} which involves the formation of metal acetylide upon deprotonation. The

proposed mechanism entails the intermediacy of a π -metal-alkyne complex that makes more acidic the acetylenic proton for subsequent abstraction and formation of the σ -metal complex, which would react with the imine or iminium ion. *In situ* formation of Au(0)^{27a} or Au(I)^{20a} nanoparticles from the gold(I)/gold(III) complexes has been claimed in some cases. Zhang and Corma reported in 2008 that Au NPs supported on ceria or zirconia catalyze the A³ coupling very efficiently.²⁸ They postulated that Au(III)/Au(I) species stabilized by the support were the active catalytic sites. Gold catalysts immobilized in metal-organic frameworks (MOFs) containing Au(0) NPs and a fraction of Au³⁺ species have also been used for the synthesis of propargylamines.²⁹ Other recent examples of gold nanoparticles in different supports as heterogeneous catalysts for this three-component reaction have been found in the literature.^{20b, 20d, 30} In one case, the A³-multicomponent reaction was performed as a two-step process,^{30a} and in two other cases under photochemical activation.^{20d, 30e} Some of these authors have confirmed a zerovalent state for the gold nanoparticles by XPS analysis.^{20b, 20d, 30d, 30f-h} However, scarce precedents exist with non-supported Au(0) NPs,³¹ two of them using aqueous extracts of flowers^{31a, 31b} and another one involving a reverse micelle system with Triton X-100 as surfactant.^{31c} Oxidized copper nanoparticles³² and Ag NPs³³ have also been reported to catalyze the A³ coupling reaction.

Taking the reaction of benzaldehyde, **5a** (1 mmol), morpholine, **6a** (1.3 mmol) and phenylacetylene, **7a** (1.3 mmol) as a model, initial attempts with **M1A-B** and **M2** (at 0.5 mol% of Au loading) were performed in water at 100 °C (in open or closed vessels) under two different concentrations (0.3 and 1 M). No evolution was observed with **M1A-B** after one day and the reaction was sluggish with **M2**. Fortunately, the propargylamine **8aaa** was satisfactorily obtained with **M2** under neat conditions at 100 °C in a closed vessel (84% by ¹H NMR) (Scheme 3).

Next, we investigated the performance of **M2** using other cyclic and acyclic secondary amines such as piperidine, **6b**, *N*-benzylmethylamine, **6c**, diethylamine, **6d**, and pyrrolidine, **6e**, affording good yields of the products **8aba**, **8aca**, **8ada** and moderate yield of **8aea**. Nanomaterials **M1A** and **M1B** were found to be less active than **M2** and provided **8aba** in 58 and 36% yield, respectively, under the same conditions. The catalyst **M2** was recovered in the synthesis of **8aca** by precipitation with diethyl ether, centrifugation and decantation, and was successfully reused for three more consecutive runs (97, 93 and 89% yield) (Scheme 3). Unexpectedly, the XPS of the recycled **M2** showed a lower proportion of Au(I) species than the fresh one, which could explain the slight decrease in activity upon reuse (see figure S3 in supporting information).



[a] **5** (0.5 mmol), **6** (0.65 mmol), **7** (0.65 mmol), in a closed vessel of 4 mL

[b] Yield determined by ¹H NMR using 4-methoxyphenol as internal standard

[c] Recycling: 97% (2nd run), 93% (3rd run), 89% (4th run)

[d] **5a** (1 mmol), **6e** (2 mmol), **7a** (1.25 mmol)

[e] In a closed vessel of 15 mL

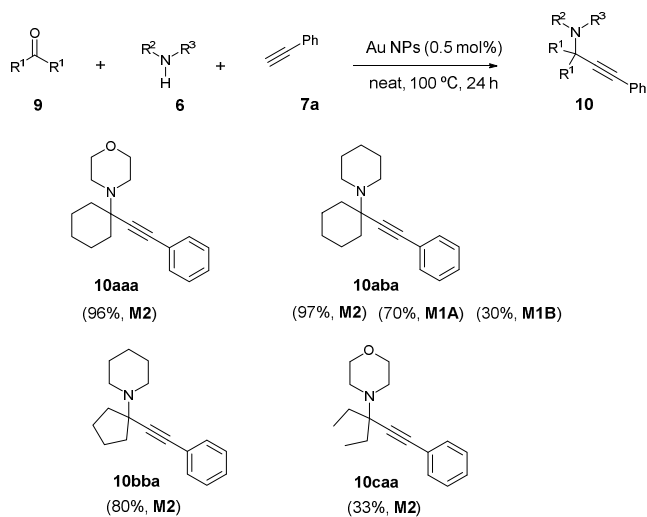
[f] Isolated yield

[g] **5a** (1 mmol), **6b** (1.25 mmol), **7b** (2 mmol)

Scheme 3. A³ coupling between aldehydes, amines and alkynes catalysed by Au NPs.^[a, b]

Aromatic aldehydes with electron-donor groups, such as *p*-methylbenzaldehyde, **5b**, and *p*-methoxybenzaldehyde, **5c**, reacted successfully with piperidine, **6b**, and phenylacetylene, **7a**, giving rise to **8bba** and **8cba** in 98 and 85% yields, respectively. In contrast, the reaction of *p*-nitrobenzaldehyde with the same reagents occurred with low conversion (not isolated). The treatment of benzaldehyde, **5a**, and piperidine, **6b**, with cyclohexylacetylene, **7b**, gave also a poor result (**8abb**, 20%). The electronic effect of substitution on the aryl ring of the alkyne was investigated by treating benzaldehyde, **5a**, and piperidine, **6b**, with *p*-methoxyphenylacetylene, **7c**, and *p*-fluorophenylacetylene, **7d**, to afford **8abc** and **8abd** in 94 and 54% yields, respectively. Aliphatic aldehydes such as *n*-butanal, **5d**, and *n*-decanal, **5e**, reacted also well with piperidine, **6b**, and phenylacetylene, **7a**, to give **8dba** and **8eba** in 89 and 83% yields, respectively (Scheme 3).

Cyclic (cyclohexanone, **9a**, cyclopentanone, **9b**) and acyclic (3-pentanone, **9c**) ketones were also coupled with secondary amines (morpholine, **6a**, piperidine, **6b**) and phenylacetylene, **7a**, at 100 °C in the absence of solvent (Scheme 4). Catalyst **M2** exhibited higher activity than **M1A** and **M1B** in the formation of **10aba** (97%, 70% and 30% yield) (Scheme 4).



[a] **9** (0.65 mmol), **6** (0.5 mmol), **7a** (0.65 mmol), in a closed vessel of 4 mL
 [b] Yield determined by ¹H NMR using 4-methoxyphenol as internal standard

Scheme 4. A³ coupling between ketones, amines and alkynes catalysed by Au NPs.^[a, b]

The differential reactivity of **M2**, **M1A** and **M1B** in the A³ coupling processes may be attributed, in part, to the content of monovalent Au(I) in the nanomaterials (as shown in the XPS spectra, **M2** contains the higher amount of Au⁺ species and shows better catalytic activity than **M1A/M1B** for **8aba** and **10aba**). Moreover, an influence of the structural features of cationic and anionic moieties of the stabilizers has also been found (if we compare the yields for **8aba** and **10aba**, **M2** with tris-imidazolium cation gives better performance than **M1A** with imidazolium cation, and **M1A** with bromide anion is better as catalyst than **M1B** with tetrafluoroborate anion). Thus, the sum of the three factors seem to determine the catalytic performance. In fact, the effect of the anion (halide or tetrafluoroborate) in the catalytic activity of Pd NPs stabilized by other tris-imidazolium salts had also been previously observed.^{7a,7c}

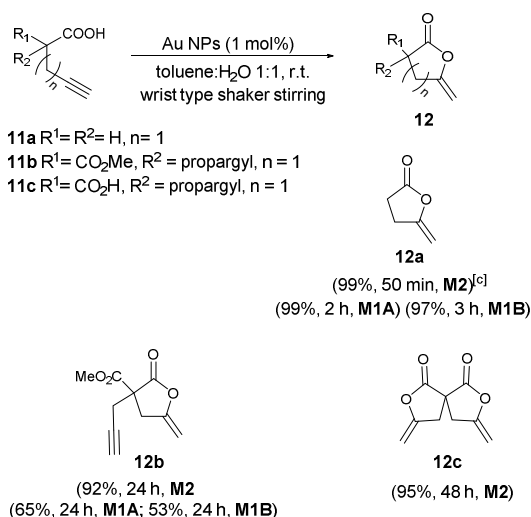
The three-component coupling of benzaldehyde, phenylacetylene and piperidine to give **8aba** has been described with commercial AuCl (1 mol%, water, 100 °C, 12 h, 99 % conversion), AuX₃ (X = Cl, Br; 1 mol%, water, 100 °C, 12 h, 100 % conversion). Under analogous conditions, with commercial Au(0) sponge (3 mol%, water, 100 °C, 12 h), there was no conversion.^{27c} Solvent effects were found for the same reaction performed with commercial AuClPPh₃ (1 mol%, 24 h) giving variable conversions (75% in water at 100 °C; 100% in 2,2,2-trifluoroethanol at 60 °C).^{27d}

Activity of gold nanoparticles in the cycloisomerization of γ -alkynoic acids into enol-lactones.

Article Online
DOI: 10.1039/D0NJ00284D

The cycloisomerization of γ -alkynoic acids into γ -alkylidene lactones has been accomplished under catalysis by NHC-Au(I) complexes³⁴ among other metal species.³⁵ Michelet has described the activity of heterogeneous gold catalysts supported in zeolite beta-NH₄⁺ in this transformation, cationic gold species being proposed to play a key role (*in situ* XPS).³⁶ More recently, Bäckvall has reported this reaction by using Au(0) nanoparticles supported in siliceous mesocellular foam and mesoporous silica nanoparticles.³⁷ Other cycloisomerization processes with substrates bearing an alkyne or allene moiety have been performed with supported gold NPs,³⁸ including aryl propargyl ethers,^{38a} 1,6-enynes,^{38b} 2-alkynylanilines,^{38c} Ugi adducts,^{38d,e} conjugated allenones,^{38f} propargylic ureas,^{38g} and allenic acids.^{38h}

After some experimentation, the cycloisomerization of 4-pentynoic acid (**11a**, [**11a**] = 0.15 M) to the lactone **12a** was best performed in a 1:1 water/toluene mixture at room temperature under catalysis by Au NPs (1 mol% Au loading) (Scheme 5). These biphasic conditions had been applied satisfactorily to this transformation when using water-soluble^{34a} and silica-supported NHCAuCl^{34c} complexes. The use of a wrist-type shaker stirring (rocking mixer vibromatic) enable an optimal mixing of the immiscible layers, which is not achieved by standard magnetic stirring. To our delight, the five-membered enol-lactone **12a** (5-exo-dig product) was formed in a nearly quantitative yield with **M2**. With the other nanocatalysts longer reaction times were required for completion of the reaction (99% yield of **12a** after 2 h for **M1A**, 97% after 3 h for **M1B**). Moreover, **M2** could be recycled successfully up to six runs (99, 96, 92, 95, 90, 88% yield) (Scheme 5). As the Au NPs remained in the aqueous phase (dark maroon colour) and the product in the organic phase (colourless), a simple decantation allowed the separation and we directly reused the aqueous layer in the subsequent cycle.



[a] **11** (0.3 mmol), toluene:H₂O 1:1 (2 mL), in a closed vessel of 4 mL
 [b] Yield determined by ¹H NMR using 4-methoxyphenol as internal standard
 [c] Recycling: 96% (2nd run), 92% (3rd run), 95% (4th run), 90 (5th run), 88 (6th run)

Scheme 5. Cycloisomerization of γ -alkynoic acids catalysed by Au NPs.^[a, b]

Encouraged by these results, other alkyynoic acids **11b-c** were subjected to the title reaction under the same conditions. The monomethyl ester **11b** cycloisomerized to the α -disubstituted lactone **12b** (92, 65 and 53% yield with **M2**, **M1A** and **M1B**, respectively, after 24 h) and the dipropargylmalonic acid **11c** afforded the spiranic dilactone **12c** (95%, 48 h, **M2**) through a double cycloisomerization process. It is worth to mention the chemoselectivity offered by the catalysts in this biphasic medium, as byproducts derived from alkyne hydration were not observed despite the presence of water.

An interesting extension of this work to be undertaken in the future is the study of other substrates/nucleophiles, such as the cycloisomerization of allenic acids^{38h} or the intramolecular addition of alcohols to alkynes, alkenes and allenes.^{35b}

Conclusions

We have synthesized new imidazolium (**S1A-B**, bromide and tetrafluoroborate) and tris-imidazolium (**S2**, bromide) salts bearing polyoxyethylenated chains through triazole-containing linkers. We have used them as stabilizers for the preparation of water-soluble gold nanoparticles, **M1A-B** and **M2**, by reduction of tetrachloroauric acid with sodium borohydride in water at room temperature. The nanomaterials have been characterized (TEM, EDS, ED, XPS, UV-Vis, ICP-OES). The XPS spectra indicated the presence of two valence states of gold, namely Au(I) and Au(0), the oxidized form being more abundant in **M2** than in **M1A-B**. The ¹H NMR spectrum of **M1B** clearly shows the presence of the C-2 imidazolic proton. In the case of **M1A** and **M2**, the absence of this and other protons of the core of the stabilizers indicates a more strong interaction with the gold surface. The catalytic activity of these nanomaterials has been tested in the A³ coupling between aldehydes (and ketones), terminal alkynes and amines under neat conditions to afford propargylamines, and in the cycloisomerization of γ -alkynoic

acids to enol lactones in a biphasic system toluene-water, at room temperature. **M2** was found to be the best catalyst and it has been recycled in both reactions (up to four and six runs, respectively) taking advantage of its solubility in water and insolubility in diethyl ether.

Experimental Section

Experimental details

Commercial reagents were used directly as received. Milli-Q water and HPLC grade solvents were used in the preparation and purification of products. The NMR spectra were recorded with Bruker Avance DRX-250 (250 MHz for ¹H), Bruker Avance DPX-360 MHz (360 MHz for ¹H) and Bruker Avance III 400SB (400 MHz for ¹H) spectrometers. ICP-OES measurements of gold content were carried out at the *Servei d'Anàlisi Química* of the *Universitat Autònoma de Barcelona* with a Perkin-Elmer instrument, model Optima 4300DV. High resolution mass spectra were performed at the *Servei d'Anàlisi Química* of the *Universitat Autònoma de Barcelona* using a Bruker Daltonics MicroTOFQ spectrometer (Bremen, Germany) equipped with an ESI inlet. Absorption spectra were recorded on an Agilent 8453 spectrophotometer by using 1 cm thick quartz cuvettes. TEM, ED and EDX analyses were performed at the *Servei de Microscòpia* of the *Universitat Autònoma de Barcelona*, with a JEOL JEM-2011 model instrument operating at 200 kV. The nanoparticle sizes were determined by measuring 500-1000 particles using Image J (Fiji) program and were subsequently averaged to produce the mean NP diameter. XPS measurements were performed at room temperature with a SPECS PHOIBOS 150 hemispherical analyzer (SPECS GmbH, Berlin, Germany) in ultra-high vacuum conditions (base pressure of 5x10⁻¹⁰ mbar) using monochromatic Al K α radiation (1486.74 eV) as excitation source. The PEGylated azide **2**,^{10b, 11} the C3-symmetric tris-imidazole **3**,^{7a, 16} and diynes **11c**,^{34c} **11d**³⁹ were prepared as described previously.

Synthesis of 1,3-di(2-propyn-1-yl)imidazolium bromide **1a**

Propargyl bromide (17.8 mL; 80 wt% in toluene; d = 1.335 g/mL; 160 mmol) was added into a round bottom flask containing *N*-(trimethylsilyl)imidazole (7.34 mL; 7.013 g; 50 mmol) under inert atmosphere. The mixture was heated under stirring at 50 °C. Upon completion of the reaction (24 h) the solid obtained was filtered, washed with Et₂O (3 x 30 mL) and dried under vacuum. The product **1a** was obtained as a white hygroscopic solid (10.59 g; 94 %; mp 123-125 °C). ¹H NMR (250 MHz, CD₃CN) δ (ppm): 9.49 (s, 1H, NCHN), 7.60 (s, 2H, NCH=CHN), 5.17 (d, *J* = 2.5 Hz, 4H; 2 x CH₂C \equiv CH), 3.06 (t, *J* = 2.5 Hz, 2H, 2 x CH₂C \equiv CH). ¹³C NMR (62.5 MHz, CD₃CN) δ (ppm): 123.4 (NCHN), 118.3 (NCH=CHN) (masked by solvent), 78.4 (CH₂C \equiv CH), 75.5 (CH₂C \equiv CH), 40.2 (NCH₂C \equiv CH). HRMS-ESI (m/z) calculated for C₉H₉N₂⁺: 145.0760; found: 145.0761.

Synthesis of 1,3-di(2-propyn-1-yl)imidazolium tetrafluoroborate **1b**

A mixture of **1a** (2.88 g, 12.8 mmol) and NaBF₄ (1.41 g, 12.84 mmol) in acetone (30 mL) was stirred at room temperature. After 24 h of reaction the mixture was filtered and the resultant solid was washed with Et₂O (2 x 50 mL). All of the organic layers were combined and the solvent was evaporated under reduced pressure. The product **1b** was obtained as a pale yellow solid (2.71 g, 91 %, mp 66 - 68 °C; lit.¹³

mp 67 °C). ¹H NMR (250 MHz, CD₃CN) δ (ppm): 8.81 (s, 1H, NCHN), 7.55 (s, 2H, NCH=CHN), 5.03 (d, *J* = 2.5 Hz, 4H; 2 x CH₂C≡CH), 3.05 (t, *J* = 2.5 Hz, 2H, 2 x CH₂C≡CH). ¹³C NMR (62.5 MHz, CD₃CN) δ (ppm): 136.6 (NCHN), 123.5 (NCH=CHN), 78.5 (CH₂C≡CH), 75.2 (CH₂C≡CH), 40.3 (NCH₂C≡CH).

Synthesis of PEG-tagged stabilizer S1A

Imidazolium salt **1a** (0.30 g, 1.33 mmol), azide **2** (3.63 g, 1.78 mmol), sodium ascorbate (0.14 g, 0.76 mmol) and copper(II) sulfate pentahydrate (0.089 g, 0.35 mmol) were dissolved in methanol (10 mL), previously degassed, and the solution was purged with N₂ flow for 10 min. The mixture was stirred in the dark, at room temperature, for 24 h under inert atmosphere. Then the solvent was evaporated under reduced pressure and the solid residue was dissolved in water. The aqueous layer was extracted with CH₂Cl₂ (4 x 20 mL) and the organic phase was washed with water (4 x 20 mL), dried with anhydrous Na₂SO₄ and filtered. The solvent was evaporated under reduced pressure obtaining **S1A** as a pale brown solid (3.13 g, 86%). ¹H NMR (250 MHz, CDCl₃) δ (ppm): 10.51 (s, 1H, NCHN), 8.37 (s, 2H, NCH=CHN), 7.59 (s, 2H, 2 x triazole-H), 5.67 (s, 4H, 2 x NCH₂-triazole), 4.55 (t, *J* = 5 Hz, 4H, 2 x NCH₂-PEG), 3.94-3.65 (m, 2 x CH₂ PEG chains), 3.40 (m, 6H, 2 x OCH₃). MS-ESI-TOF (*m/z*): peaks between 3519.3 and 4445.0 corresponding to [M]⁺ separated by 44 D (CH₂CH₂O); the most intense peak at 4047.7 (86 CH₂CH₂O units + C₉H₉N₈ nitrogen-rich core + 2 CH₃).

Synthesis of PEG-tagged stabilizer S1B

Imidazolium salt **1b** (55 mg, 0.22 mmol), azide **2** (883 mg, 0.43 mmol), sodium ascorbate (34.9 mg, 0.18 mmol) and copper(II) sulfate pentahydrate (21.5 mg, 0.09 mmol) were dissolved in methanol (10 mL), previously degassed, and the solution was purged with N₂ flow for 10 min. The mixture was stirred in the dark, at room temperature, for 3 days under inert atmosphere. Then the mixture was filtered through Celite and washed with MeOH (20 mL) and CH₂Cl₂ (20 mL). The organic phase was dried with anhydrous Na₂SO₄, filtered and the solvent was evaporated under reduced pressure. The obtained residue was washed with Et₂O and dried under vacuum obtaining **S1B** as a pale yellow solid (783 mg, 84 %). ¹H NMR (360 MHz, CDCl₃) δ (ppm): 9.19 (s, 1H, NCHN), 8.25 (s, 2H, NCH=CHN), 7.54 (s, 2H, 2 x triazole-H), 5.52 (s, 4H, 2 x NCH₂-triazole), 4.56 (t, *J* = 5 Hz, 4H, 2 x NCH₂-PEG), 3.87 – 3.44 (m, 2 x CH₂ PEG chains), 3.37 (m, 6H, 2 x OCH₃). MS-ESI-TOF (*m/z*): peaks between 3474.3 and 4267.1 corresponding to [M]⁺ separated by 44 D (CH₂CH₂O); the most intense peak at 3870.4 (82 CH₂CH₂O units + C₉H₉N₈ nitrogen-rich core + 2 CH₃).

Synthesis of 1,1',1''-[(2,4,6-trimethylbenzene-1,3,5-triyl)-tris(methylene)]tris(3-propargyl-1H-imidazol-3-ium) bromide **4**

Propargyl bromide (1.4 mL; 80 wt% in toluene; *d* = 1.335 g/mL; 15.7 mmol) was added to a solution of **3** (0.452 g; 1.25 mmol) in a 2:1 toluene/acetonitrile mixture (9 mL). The reaction mixture was stirred at 50 °C under inert atmosphere for 24 h. Then Et₂O was added until a fine solid precipitated, which was separated by decantation, washed with Et₂O and dried to obtain **4** (0.77 g, 63 %). ¹H NMR (360 MHz, (CD₃)₂SO) δ (ppm): 9.28 (s, 3H, N=CHN), 7.88 (s, 3H, C=CHN), 7.81 (s, 3H, C=CHN), 5.59 (s, 6H, CH₂), 5.24 (s, 6H, CH₂), 3.82 (s, 3H, ≡CH), 2.30 (s, 9H, CH₃). ¹³C NMR (360 MHz, (CD₃)₂SO) δ (ppm): 141.2

(Ph), 135.7 (N=CN), 129.3 (Ph), 122.9 (NCH=), 122.3 (NCH=), 78.7 (C≡), 76.3 (≡CH), 48.0 (CH₂), 16.4 (CH₃). HRMS-ESI-TOF (*m/z*) calculated for C₃₀H₃₃Br₂N₆⁺: 635.1128; found: 635.1115.

Synthesis of PEG-tagged stabilizer S2

Tris-imidazolium salt **4** (0.201 g, 0.28 mmol), azide **2** (1.883 g, 0.92 mmol), sodium ascorbate (0.131 g, 0.663 mmol) and copper(II) sulfate pentahydrate (0.077 g, 0.308 mmol) were dissolved in a previously degassed 1:1 MeOH:water mixture (3.2 mL). The solution was purged with a N₂ flow for 10 min and then was stirred in the dark at 50 °C for 24 h under inert atmosphere. The mixture was centrifuged and the methanol from the supernatant was evaporated at reduced pressure. The aqueous residue was extracted with CH₂Cl₂ (4 x 20 mL) and the organic phase was washed with water (3 x 20 mL). Then, the organic layer was dried over anhydrous Na₂SO₄, filtered and the solvent was evaporated to obtain a brownish oily residue. Then, Et₂O was added until a solid was precipitated, which was filtered and washed with Et₂O to obtain **S2** (1.504 g, 79 %, mp = 52 - 53 °C). ¹H NMR (360 MHz, CDCl₃) δ (ppm): 10.21 (br s, 3H, N=CHN), 8.29 (br s, 3H, NCH=), 7.89 (br s, 3H, C=CHN), 7.56 (br s, 3H, C=CHN), 5.75 (br s, 6H, CH₂), 5.62 (br s, 6H, CH₂), 4.54 (m, 6H), 3.90-3.38 (m, CH₂ of PEG chains), 3.38 (s, 9H, -OCH₃), 2.43 (br s, 9H, -CH₃). MS-MALDI-TOF (*m/z*): peaks between 1685.650 (33 CH₂CH₂O units + C₃₀H₃₃N₁₅ nitrogen-rich core + 3 CH₃) and 2253.907 (46 CH₂CH₂O units + C₃₀H₃₃N₁₅ nitrogen-rich core + 3 CH₃) corresponding to [M]³⁺ separated by 44 D (CH₂CH₂O unit); the most intense peak at 1903.742 (38 CH₂CH₂O units + C₃₀H₃₃N₁₅ nitrogen-rich core + 3 CH₃).

Synthesis of Au NPs M1A stabilized by S1A

Stabilizer **S1A** (77.5 mg; 0.018 mmol) and tetrachloroauric acid trihydrate (24 mg; 0.06 mmol) were dissolved in distilled water (100 mL) under inert atmosphere to afford a yellow solution. Then, 4 mL of 0.1 M NaBH₄ solution (0.4 mmol) were added dropwise for 2 min. The reaction mixture turned deep red and was stirred at room temperature overnight. After this time, the mixture was filtered through a Milli-Pore filter (0.2 μm, nylon) and then extracted with CH₂Cl₂ (6 x 30 mL). The organic phase was dried over anhydrous Na₂SO₄, filtered and then the solvent was evaporated to obtain the Au NPs **M1A** as a dark red powder (85.6 mg, 10.9 % Au (ICP-OES), 79 % yield according to the starting Au).

Synthesis of Au NPs M1B stabilized by S1B

Stabilizer **S1B** (77.6 mg; 0.018 mmol) and tetrachloroauric acid trihydrate (24 mg; 0.06 mmol) were dissolved in distilled water (100 mL) under inert atmosphere to afford a yellow solution. Then, 4 mL of 0.1 M NaBH₄ solution (0.4 mmol) were added dropwise for 2 min. The reaction mixture turned deep red and was stirred at room temperature overnight. After this time, the mixture was filtered through a Milli-Pore filter (0.2 μm, nylon) and then extracted with CH₂Cl₂ (6 x 30 mL). The organic phase was dried over anhydrous Na₂SO₄, filtered and then the solvent was evaporated to obtain the Au NPs **M1B** as a dark red powder (85.5 mg, 9.5 % Au (ICP-OES), 68.7 % yield according to the starting Au).

Synthesis of Au NPs M2 stabilized by S2

Stabilizer **S2** (133.6 mg; 0.02 mmol) and tetrachloroauric acid trihydrate (23.6 mg; 0.06 mmol) were dissolved in distilled water

(100 mL) under inert atmosphere to afford a yellow solution. Then, 4 mL of 0.1 M NaBH₄ solution (0.4 mmol) were added dropwise for 2 min. The reaction mixture turned deep red and was stirred at room temperature overnight. After this time, the mixture was filtered through a Milli-Pore filter (0.2 μm, nylon) and then extracted with CH₂Cl₂ (6 x 30 mL). The organic phase was dried over anhydrous Na₂SO₄, filtered and then the solvent was evaporated to obtain the Au NPs **M2** as a dark red powder (117.9 mg, 6.9 % Au (ICP-OES), 68.8 % yield according to the starting Au).

General procedure for the synthesis of propargylamines via A³ coupling between aldehydes, secondary amines and alkynes

Aldehyde (1 equiv), secondary amine (1.3 equiv), alkyne (1.3 equiv) and Au NPs (0.5 mol% Au) were mixed into a sealed tube in the absence of solvent. The mixture was stirred at 100 °C for 24 h. After that time, 1 equiv of 4-methoxyphenol as internal standard was added and the yield of propargylamine was determined by ¹H RMN. In order to isolate the product, water was added to the mixture and the solution was extracted with Et₂O (3 x 5 mL). The organic layer was dried over anhydrous Na₂SO₄, filtered and the solvent evaporated under reduced pressure. A sample of pure product was obtained after flash chromatography on alumina (10:0.1 hexane:EtOAc). For the recycling of the catalyst, the Au NPs were recovered by addition of diethyl ether to the crude mixture, centrifugation and decantation. The solid insoluble in diethyl ether was reused in the next run. The ethereal phase was washed with water, dried over anhydrous Na₂SO₄ and the solvent was evaporated to give the corresponding propargylamine.

General procedure for the synthesis of propargylamines via A³ coupling between ketones, secondary amines and alkynes

Ketone (1.3 equiv), secondary amine (1 equiv), alkyne (1.3 equiv) and Au NPs (0.5 mol % Au) were mixed into a sealed tube in the absence of solvent. The mixture was stirred at 100 °C for 24 h. After that time, 1 equiv of 4-methoxyphenol was added as internal standard and the yield of propargylamine was determined by ¹H RMN. In order to isolate the product water was added to the mixture and the solution was extracted with Et₂O (3 x 5 mL). The organic layer was dried over Na₂SO₄, filtered and the solvent evaporated under reduced pressure. A sample of pure product was obtained after flash chromatography on alumina (10:0.1 hexane:EtOAc).

General procedure for the cycloisomerization of γ-alkynoic acids into enol lactones

To a biphasic system of toluene/water 1:1 (1 mL), the corresponding γ-alkynoic acid (0.15 mmol) and Au NPs (1 mol %, 0.0015 mmol of Au) were added. The resulted mixture was stirred with a wrist type laboratory shaker apparatus at room temperature until complete conversion of alkynoic acid (monitored by ¹H NMR using 4-methoxyphenol as internal standard). The organic phase was then separated and the aqueous layer was washed with Et₂O (3x1 mL). The combined organic layers were dried over anhydrous Na₂SO₄, filtered and the solvent was evaporated. The obtained residue was then purified by flash chromatography (hexane: AcOEt, 80:20) to obtain the desired enol lactone.

Conflicts of interest

There are no conflicts to declare.

View Article Online
DOI: 10.1039/D0NJ00284D

Acknowledgements

We are thankful for financial support from *Ministerio de Economía, Industria y Competitividad* (MINECO) of Spain (Projects CTQ2014-53662-P and CTQ2016-81797-REDC), *Ministerio de Ciencia, Innovación y Universidades* (MCINN) of Spain (Project RTI2018-097853-B-I00), *DURSI-Generalitat de Catalunya* (SGR2017-0465), and *Universitat Autònoma de Barcelona* for predoctoral scholarship to G. F.

Notes and references

- a) E. C. Dreaden, M. A. Mackey, X. Huang, B. Kang, M. A. El-Sayed, *Chem. Soc. Rev.*, 2011, **40**, 3391-3304; b) E. C. Dreaden, A. M. Alkilany, X. Huang, C. J. Murphy, M. A. El-Sayed, *Chem. Soc. Rev.*, 2012, **41**, 2740-2779; c) I. Fratoddi, I. Venditti, C. Cametti, M. V. Russo, *J. Mater. Chem. B.*, 2014, **2**, 4204-4220; d) W. Zhou, X. Gao, D. Liu, X. Chen, *Chem. Rev.*, 2015, **115**, 10575-10636; e) J. R. Melamed, R. S. Riley, D. M. Valcourt, E. S. Day, *ACS Nano* 2016, **10**, 10631-10635; f) C-C. Wang, S-M. Wu, H-W. Li, H-T. Chang, *ChemBioChem*, 2016, **17**, 1052-1062; g) J. Li, J. Liu, C. Chen, *ACS Nano*, 2017, **11**, 2403-2409; h) J. Zong, S. L. Cobb, N. R. Cameron, *Biomater. Sci.*, 2017, **5**, 872-886; i) G. Bodelón, C. Costas, J. Pérez-Juste, I. Pastoriza-Santos, L. M. Liz-Marzán, *Nano Today*, 2017, **13**, 40-60; j) T. Aghaie, M. Hadi Jazayeri, M. Manian, I. Khani, M. Erfani, M. Rezayi, G. A. Ferns, A. Avan, *J. Cell. Biochem.*, 2019, **120**, 2749-2755; k) M. Yadid, R. Feiner, T. Dvir, *Nano Lett.*, 2019, **19**, 2198-2206; l) K. Sztandera, M. Gorzkiewicz, B. Klajnert-Maculewicz, *Mol. Pharmaceutics*, 2019, **16**, 1-23; m) A. Artiga, I. Serrano-Sevilla, L. De Matteis, S. G. Mitchell, J. M. de la Fuente, *J. Mater. Chem. B*, 2019, **7**, 876-896; n) J. Beik, M. Khateri, Z. Khosravi, S. Kamran Kamrava, S. Kooranifar, H. Ghaznavi, A. Shakeri-Zadeh, *Coord. Chem. Rev.*, 2019, **387**, 299-324; o) P. Khandelwal, D. K. Singh, P. Poddar, *ChemistrySelect*, 2019, **4**, 6719-6738; p) J. Olesiak-Banska, M. Waszkielewicz, P. Obstarczyk, M. Samoc, *Chem. Soc. Rev.*, 2019, **48**, 4087-4117; q) M. Yu, J. Xu, J. Zheng, *Angew. Chem. Int. Ed.*, 2019, **58**, 4112-4128.
- a) K. M. Mayer, J. H. Hafner, *Chem. Rev.*, 2011, **111**, 3828-3857; b) K. Saha, S. S. Agasti, C. Kim, X. Li, V. M. Rotello, *Chem. Rev.*, 2012, **112**, 2739-2779; c) H. Jans, Q. Huo, *Chem. Soc. Rev.*, 2012, **41**, 2849-2866; d) G. Yue, S. Su, N. Li, M. Shuai, X. Lai, D. Astruc, P. Zhao, *Coord. Chem. Rev.*, 2016, **311**, 75-84; e) L. Qin, G. Zeng, C. Lai, D. Huang, P. Xu, C. Zhang, M. Cheng, X. Liu, S. Liu, Bi. Li, H. Yi, *Coord. Chem. Rev.*, 2018, **359**, 1-31; f) P. Jiang, Y. Wang, L. Zhao, C. Ji, D. Chen, L. Nie, *Nanomaterials*, 2018, **8**, 977; g) H. Chen, K. Zhou, G. Zhao, *Trends Food Sci. Technol.*, 2018, **78**, 83-94; h) H. Aldewachi, T. Chalati, M. N. Woodrooffe, N. Bricklebank, B. Sharrack, P. Gardiner, *Nanoscale*, 2018, **10**, 18-33; i) C-C. Chang, C-P. Chen, T-H. Wu, C-H. Yang, C-W. Lin, C-Y. Chen, *Nanomaterials*, 2019, **9**, 861; j) C. Coutinho, A. Somoza, *Anal. Bioanal. Chem.* 2019, **411**, 1807-1824.
- a) A. Corma and H. García, *Chem. Soc. Rev.*, 2008, **37**, 2096-2126; b) M. Stratakis and H. García, *Chem. Rev.*, 2012, **112**, 4469-4506; c) X. Zhang and Y. Ding, *Catal. Sci. Technol.*, 2013, **3**, 2862-2868; d) Y. Mikami, A. Dhakshinamoorthy, M. Alvaro and H. García, *Catal. Sci. Technol.*, 2013, **3**, 58-69; e) T. Mitsudome, K. Kaneda, *Green Chem.* 2013, **15**, 2636-2654; f) B. S. Takale, M. Bao and Y. Yamamoto, *Org. Biomol. Chem.*, 2014, **12**, 2005-2027; g) M. Boronat, A. Leyva-Pérez, A. Corma, *Acc. Chem. Res.* 2014, **47**, 834-844; h) P. Serna, A.

Corma, *ACS Catal.*, 2015, **5**, 7114-7121; i) J. Zhao, L. Ge, H. Yuan, Y. Liu, Y. Gui, B. Zhang, L. Zhou, S. Fang, *Nanoscale*, 2019, **11**, 11429-11436; j) Y. Hui, S. Zhang, W. Wang, *Adv. Synth. Catal.*, 2019, **361**, 2215-2235; k) J. M. Campelo, D. Luna, R. Luque, J. M. Marinas, A. A. Romero, *ChemSusChem*, 2009, **2**, 18-45; l) G. Li, R. Jin, *Nanotechnol. Rev.*, 2013, **2**, 529-545; m) M. Nasrollahzadeh, M. Sajjadi, F. Ghorbannezhad, S. Mohammad Sajadi, *Chem. Rec.*, 2018, **18**, 1409-1473.

4 a) H. Tsunoyama, H. Sakurai, Y. Negishi, T. Tsukuda, *J. Am. Chem. Soc.*, 2005, **127**, 9374-9375; b) Y. Piao, Y. Jang, M. Shokouhimehr, I. Su Lee, T. Hyeon, *Small*, 2007, **3**, 255-260.

5 A. Roucoux, J. Schulz, H. Patin, *Chem. Rev.*, 2002, **102**, 3757-3778.

6 a) D. X. Li, Q. He, Y. Cui, J. B. Li, *Chem. Mater.*, 2007, **19**, 412-417; b) H. Huang, X. Yang, *Biomacromolecules*, 2004, **5**, 2340-2346; c) X. P. Sun, S. J. Dong, E. K. Wang, *Polymer*, 2004, **45**, 2181-2184; d) A. Gole, C. J. Murphy, *Chem. Mater.*, 2005, **17**, 1325-1330; e) M. Q. Zhu, L. Q. Wang, G. J. Exarhos, A. D. Q. Li, *J. Am. Chem. Soc.*, 2004, **126**, 2656-2657; f) M. Ortega-Muñoz, V. Blanco, F. Hernández-Mateo, F. J. López-Jaramillo, F. Santoyo-González, *ChemCatChem*, 2017, **9**, 3965-3973; g) J. Lü, Y. Fang, J. Gao, H. Duan, C. Lü, *Langmuir*, 2018, **34**, 8205-8214; h) S. Doherty, J. G. Knight, T. Backhouse, R. J. Summers, E. Abood, W. Simpson, W. Paget, R. A. Bourne, T. W. Chamberlain, R. Stones, K. R. J. Lovelock, J. M. Seymour, M. A. Isaacs, C. Hardacre, H. Daly, N. H. Rees, *ACS Catal.*, 2019, **9**, 4777-4791.

7 a) M. Planellas, R. Pleixats, A. Shafir, *Adv. Synth. Catal.*, 2012, **354**, 651-662; b) M. Planellas, Y. Moglie, F. Alonso, M. Yus, R. Pleixats, A. Shafir, *Eur. J. Org. Chem.*, 2014, 3001-3008; c) M. Planellas, W. Guo, F. Alonso, M. Yus, A. Shafir, R. Pleixats, T. Parella, *Adv. Synth. Catal.*, 2014, **356**, 179-188.

8 G. Fernández, J. Sort, R. Pleixats, *ChemistrySelect*, 2018, **3**, 8597-8603.

9 G. Fernández, R. Pleixats, *ChemistrySelect*, 2018, **3**, 11486-11493.

10 a) N. Mejías, A. Serra-Muns, R. Pleixats, A. Shafir, M. Tristany, *Dalton Trans*, 2009, 7748-7755; b) N. Mejías, R. Pleixats, A. Shafir, M. Medio-Simón, G. Asensio, *Eur. J. Org. Chem.*, 2010, 5090-5099.

11 W. Guo, R. Pleixats, A. Shafir, T. Parella, *Adv. Synth. Catal.*, 2015, **357**, 89-99.

12 W. Guo, R. Pleixats, A. Shafir, *Chem. Asian J.*, 2015, **10**, 2437-2443.

13 Z. Fei, D. Zhao, R. Scopelliti, P. J. Dyson, *Organometallics*, 2004, **23**, 1622-1628.

14 a) V. V. Rostovtsev, L. G. Green, V. V. Fokin, K. B. Sharpless, *Angew. Chem. Int. Ed.* 2002, **41**, 2596-2599; b) T. Devic, O. David, M. Valls, J. Marrot, F. Couty, G. Férey, *J. Am. Chem. Soc.*, 2007, **129**, 12614-12615; c) M. Meldal, C. W. Tornøe, *Chem. Rev.* 2008, **108**, 2952-3015.

15 M. J. MacLeod, J. A. Johnson, *J. Am. Chem. Soc.*, 2015, **137**, 7974-7977.

16 H.-K. Liu, W.-Y. Sun, H.-L. Zhu, K.-B. Yu, W.-X. Tang, *Inorg. Chim. Acta*, 1999, **295**, 129-135.

17 P. Zhao, N. Li, D. Astruc, *Coord. Chem. Rev.*, 2013, **257**, 638-665.

18 a) H. Itho, K. Naka, Y. Chujo, *J. Am. Chem. Soc.*, 2004, **126**, 3026-3027; b) E. Dinda, S. Si, A. Kotal, T. K. Mandal, *Chem. Eur. J.* 2008, **14**, 5528-5537; c) Z. Wang, Q. Zhang, D. Kuehner, A. Ivaska, L. Niu, *Green Chem.*, 2008, **10**, 907-909; d) M. Buaki, C. Aprile, A. Dhakshinamoorthy, M. Alvar, H. Garcia, *Chem. Eur. J.*, 2009, **15**, 13082-13089; e) I. Biondi, G. Laurency, P. J. Dyson, *Inorg. Chem.*, 2011, **50**, 8038-8045; f) H. Wender, M. L. Andrezza, R. R. B. Correia, S. R. Teixeira, J. Dupont, *Nanoscale*, 2011, **3**, 1240-1245; g) L. Casal-Dujat, M. Rodrigues, A. Yagüe, A. C. Calpena, D. B. Amabilino, J. González-Linares, M. Borràs, L. Pérez-García, *Langmuir*, 2012, **28**, 2368-2381. DOI: 10.1039/D0NJ00284D

19 a) C. J. Serpell, J. Cookson, A. L. Thompson, C. M. Brown, P. D. Beer, *Dalton Trans.*, 2013, **42**, 1385-1393; b) J. Crespo, Y. Guari, A. Ibarra, J. Larionova, T. Lasanta, D. Laurencin, J. M. López-de-Luzuriaga, M. Monge, M. E. Olmos, S. Richeter, *Dalton Trans.*, 2014, **43**, 15713-15718; c) X. Ling, S. Roland, M.-P. Pileni, *Chem. Mater.*, 2015, **27**, 414-423; d) A. Ferry, K. Schaepe, P. Tegeder, C. Richter, K. M. Chepiga, B. J. Ravoo, F. Glorius, *ACS Catal.*, 2015, **5**, 5414-5420; e) K. Salorinne, R. W. Y. Man, C.-H. Li, M. Taki, M. Nambo, C. M. Crudden, *Angew. Chem. Int. Ed.*, 2017, **56**, 6198-6202; f) M. R. Narouz, C.-H. Li, A. Nazemi, C. M. Crudden, *Langmuir*, 2017, **33**, 14211-14219; g) A.J. Young, M. Sauer, G. M. D. Rubio, A. Sato, A. Foelske, C. J. Serpell, J. Min Chin, M. R. Reithofer, *Nanoscale*, 2019, **11**, 8327-8333; h) N. Bridonneau, L. Hippolyte, D. Mercier, D. Portehault, M. Desage-El Murr, P. Marcus, L. Fensterbank, C. Chanéac, F. Ribot, *Dalton Trans.*, 2018, **47**, 6850-6859.

20 a) E. Belmonte Sánchez, M. J. Iglesias, H. el Hajjoui, L. Rocas, S. García-Granda, P. Villuendas, E. P. Urriolabeitia, F. López Ortiz, *Organometallics*, 2017, **36**, 1962-1973; b) A. Bhargava, N. Jain, S. Gangopadhyay, J. Panwar, *Process Biochem.*, 2015, **50**, 1293-1300; c) H. Zhang, H. Cui, *Langmuir*, 2009, **25**, 2604-2612; d) V. Panwar, S. L. Jain, *Mater. Sci. Eng. C*, 2019, **99**, 191-201.

21 a) P. Migowski, J. Dupont, *Chem. Eur. J.*, 2007, **13**, 32-39; b) L. S. Ott, R. G. Finke, *Inorg. Chem.*, 2006, **45**, 8382-8393.

22 The coordination with the metallic surface in the nanoparticles has been found to produce a signal decrease and/or broadening (or even disappearance) for the protons placed near the coordinating atoms. See, for instance: a) K. Naka, M. Yaguchi, Y. Chujo, *Chem. Mater.*, 1999, **11**, 849-851; b) C. Pan, K. Pelzer, K. Philippot, B. Chaudret, F. Dasenoy, P. Lecante, M.-J. Casanove, *J. Am. Chem. Soc.*, 2001, **123**, 7584-7593.

23 K. Lauder, A. Toscani, N. Scalacci, D. Castagnolo, *Chem. Rev.*, 2017, **117**, 14091-14200.

24 a) F. Xiao, Y. Chen, Y. Liu, J. Wang, *Tetrahedron*, 2008, **64**, 2755-2761; b) D. Shibata, E. Okada, J. Molette, M. Médebielle, *Tetrahedron Lett.*, 2008, **49**, 7161-7164; c) Y. Yamamoto, H. Hayashi, T. Saigoku, H. Nishiyama, *J. Am. Chem. Soc.*, 2005, **127**, 10804-10805; d) D. F. Harvey, D. M. Sigano, *J. Org. Chem.*, 1996, **61**, 2268-2272; e) B. Yan, Y. Liu, *Org. Lett.*, 2007, **9**, 4323-4326; f) E.-S. Lee, H.-S. Yeom, J.-H. Hwang, S. Shin, *Eur. J. Org. Chem.*, 2007, 3503-3507; g) C. Jiang, M. Xu, S. Wang, H. Wang, Z.-J. Yao, *J. Org. Chem.*, 2010, **75**, 4323-4325; h) F. J. Fañanas, T. Arto, A. Mendoza, F. Rodríguez, *Org. Lett.*, 2011, **13**, 4184-4187; i) T. S. Symeonidis, M. G. Kallitsakis, K. E. Litinas, *Tetrahedron Lett.*, 2011, **52**, 5452-5455; for a recent review, see ref. 23.

25 a) A. Hoepfing, K. M. Johnson, C. George, J. Flippen-Anderson, A. P. Kozikowski, *J. Med. Chem.*, 2000, **43**, 2064-2071; b) B. Jiang, M. Xu, *Angew. Chem. Int. Ed.*, 2004, **43**, 2543-2546; c) J. J. Fleming, J. Du Bois, *J. Am. Chem. Soc.*, 2006, **128**, 3926-3927.

26 a) V. A. Peshkov, O. P. Pereshivko, E. V. Van der Eycken, *Chem. Soc. Rev.*, 2012, **41**, 3790-3807; b) I. Jesin, G. Chandra Nandi, *Eur. J. Org. Chem.*, 2019, 2704-2720.

27 a) G. A. Price, A. K. Brisdon, S. Randall, E. Lewis, D. M. Whittaker, R. G. Pritchard, C. A. Muryn, K. R. Flower, *J. Organometallic Chem.*, 2017, **846**, 251-262; b) D. M. Lustosa, P. Cieslik, D. Hartmann, T. Bruckhoff, M. Rudolph, F. Rominger, A. S. Hashmi, *Org. Chem. Front.*, 2019, **6**, 1655-1662; c) C. Wei, C.-J. Li, *J. Am. Chem. Soc.*, 2003, **125**, 9584-9585; d) G. A. Price, A. K. Brisdon, K. R. Flower, R. G. Pritchard, P. Quayle, *Tetrahedron Lett.*, 2014, **55**, 151-154.

Published on 23 March 2020. Downloaded by University of Rochester on 3/23/2020 11:48:25 AM.

- 28 X. Zhang, A. Corma, *Angew. Chem. Int. Ed.*, 2008, **47**, 4358-4361.
- 29 L. Lili, Z. Xin, G. Jinsen, X. Chunming, *Green Chem.*, 2012, **14**, 1710-1720.
- 30 a) L. Abahmane, J. M. Köhler, G. A. Groß, *Chem. Eur. J.*, 2011, **17**, 3005-3010; b) K. Layek, R. Chakravarti, M. Lakshmi Kantam, H. Maheswaran, A. Vinu, *Green Chem.*, 2011, **13**, 2878-2887; c) B. Karimi, M. Gholinejad, M. Khorasani, *Chem. Commun.*, 2012, **48**, 8961-8963; d) N. Anand, P. Ramudu, K. Hari Prasad Reddy, K. Seetha, R. Rao, B. Jagadeesh, V. Sahithya Phani Babu, D. Raju Burri, *Appl. Catal. A Gen.*, 2013, **454**, 119-126; e) M. González-Béjar, K. Peters, G. L. Hallett-Tapley, M. Grenier, J. C. Scaiano, *Chem. Commun.*, 2013, **49**, 1732-1734; f) J.-L. Huang, D. G. Gray, C.-J. Li, Beilstein *J. Org. Chem.*, 2013, **9**, 1388-1396; g) B. Jyoti Borah, S. Jyoti Borah, K. Saikia, D. Kumar Dutta, *Cat. Sci. Technol.*, 2014, **4**, 4001-4009; h) S. Kazemi Movahed, M. Shariatipour, M. Dabiri, *RSC Adv.*, 2015, **5**, 33423-33431; i) A. Feiz, A. Bazgir, *Catal. Commun.*, 2016, **73**, 88-92; j) N. Hussain, M. R. Das, *New J. Chem.*, 2017, **41**, 12756-12766; k) N. Zohreh, S. Hassan Hosseini, M. Jahani, M. S. Xaba, R. Meijboom, *J. Catal.*, 2017, **356**, 255-268; l) M. Gholinejad, F. Zareh, C. Nájera, *Appl. Organometal. Chem.*, 2018, **32**, e4454; m) M. Loni, H. Yazdani, A. Bazgir, *Catal. Lett.*, 2018, **148**, 3467-3476; n) F. Matloubi Moghaddam, R. Pourkaveh, *ChemistrySelect*, 2018, **3**, 2053-2058; o) M. Gholinejad, R. Bonyasi, C. Nájera, F. Saadati, M. Bahrami, N. Dasvarz, *ChemPlusChem*, 2018, **83**, 431-438; p) Y. Wang, H. Zhang, X. Lin, S. Chen, Z. Jiang, J. Wang, J. Huang, F. Zhang, H. Li, *New J. Chem.*, 2018, **42**, 2197-2203; q) R. Soengas, Y. Navarro, M. J. Iglesias, F. López-Ortiz, *Molecules*, 2018, **23**, 2975; r) H. Aghahosseini, S. J. Tabatabaei Rezaei, M. Tadayyon, A. Ramazani, V. Amani, R. Ahmadi, D. Abdolahnjadian, *Eur. J. Inorg. Chem.*, 2018, 2589-2598.
- 31 a) M. Nasrollahzadeh, S. Mohammad Sajadi, *RSC Adv.*, 2015, **5**, 46240-46246; b) H. Veisi, M. Farokhi, M. Hamelian, S. Hemmati, *RSC Adv.*, 2018, **8**, 38186-38195; c) M. Kidwai, V. Bansal, A. Kumar, S. Mozumdar, *Green. Chem.*, 2007, **9**, 742-745.
- 32 a) M. Lakshmi Kantam, S. Laha, J. Yadav, S. Bhargava, *Tetrahedron Lett.*, 2008, **49**, 3083-3086; b) M. J. Albadalejo, F. Alonso, Y. Moglie, M. Yus, *Eur. J. Org. Chem.*, 2012, 3093-3104.
- 33 a) G-P. Yong, D. Tian, H-W. Tong, S-M. Liu, *J. Mol. Catal. A. Chem.*, 2010, **323**, 40-44; b) J. Cao, H. Tian, *Chem. Asian J.*, 2018, **13**, 1561-1569.
- 34 See, for instance: a) E. Tomás-Mendivil, P. Y. Toullec, J. Borge, S. Conejero, V. Michelet, V. Cadierno, *ACS Catal.*, 2013, **3**, 3086-3098; b) K. Belger, N. Krause, *Org. Biomol. Chem.*, 2015, **13**, 8556-8560; c) M. Ferré, X. Cattoën, M. Wong Chi Man, R. Pleixats, *ChemCatChem*, 2016, **8**, 2824-2831; d) D. Gasperini, L. Maggi, S. Dupuy, R. M. P. Veenboer, D. B. Cordes, A. M. Z. Slawin, S. P. Nolan, *Adv. Synth. Catal.*, 2016, **358**, 3857-3862; e) M. J. Rodríguez-Alvarez, C. Vidal, J. Díez, J. García-Alvarez, *Chem. Commun.*, 2014, **50**, 12927-12929.
- 35 a) For a general review covering transition-metal catalysed addition of carboxylic acids onto alkynes, see: N. T. Patil, R. D. Kavthe, V. S. Shinde, *Tetrahedron*, 2012, **68**, 8079-8146; b) for a specific review on gold-catalyzed O-H bond addition to unsaturated organic molecules, see: N. Huguet, A. M. Echavarren, *Top. Organomet. Chem.*, 2013, **43**, 291-324. Other references: c) J. García-Alvarez, J. Díez, C. Vidal, *Green Chem.*, 2012, **14**, 3190-3196; d) B. Saavedra, J. M. Pérez, M. J. Rodríguez-Alvarez, J. García-Alvarez, D. J. Ramón, *Green Chem.*, 2018, **20**, 2151-2157.
- 36 F. Neatu, Z. Li, R. Richards, P. Y. Toullec, J.-P. Genêt, K. Dumbuya, J. Michael Gottfried, H-P. Steinrück, V. I. Pârvulescu, V. Michelet, *Chem. Eur. J.*, 2008, **14**, 9412-9418.
- 37 a) K. Eriksson, O. Verho, L. Nyholm, S. Oscarsson, J.-E. Bäckvall, *Eur. J. Org. Chem.*, 2015, 2250-2255; b) Q. Verho, J. Gao, E. V. Johnston, W. Wan, A. Nagendiran, H. Zheng, J.-E. Bäckvall, X. Zou, *Appl. Mater.*, 2014, **2**, 113316.
- 38 a) C. Efe, I. N. Lykakis, M. Stratakis, *Chem. Commun.*, 2011, **47**, 803-805; b) C. Gryparis, C. Efe, C. Raptis, I. N. Lykakis, M. Stratakis, *Org. Lett.*, 2012, **14**, 2956-2959; c) J. E. Perea-Buceta, T. Wirtanen, O.-V. Laukkanen, M. K. Mäkelä, M. Nieger, M. Mechionna, N. Huittinen, J. A. López-Sánchez, J. Helaja, *Angew. Chem. Int. Ed.*, 2013, **52**, 11835-11839; d) F. Schröder, M. Ojeda, N. Erdmann, J. Jacobs, R. Luque, T. Noël, L. Van Meervelt, J. Van der Eycken, E. V. Van der Eycken, *Green Chem.*, 2015, **17**, 3314-3318; e) F. Schröder, N. Erdmann, T. Noël, R. Luque, E. V. Van der Eycken, *Adv. Synth. Catal.*, 2015, **357**, 3141-3147; f) L. Zorba, M. Kidonakis, I. Saridakis, M. Stratakis, *Org. Lett.*, 2019, **21**, 5552-5555; g) A. Zuliani, P. Ranjan, R. Luque, E. V. Van der Eycken, *ACS Sustainable Chem. Eng.*, 2019, **7**, 5568-5575; h) S. Handa, S. S. Subramaniam, A. A. Ruch, J. M. Tanski, L. M. Slaughter, *Org. Biomol Chem.* 2015, **13**, 3936-3949.
- 39 J. Alemán, V. Solar, C. Navarro-Ranninger, *Chem. Commun.* 2010, **46**, 454-456.

ARTICLE



Water-soluble gold nanoparticles prepared in the presence of PEG-tagged tris-imidazolium bromide, containing Au(0) and Au(I) species, are reusable catalysts